 DOI: 10.1002/masy.201051031

FTIR-ATR Monitoring and SEC/RI/MALLS Characterization of ATRP Synthesized Hyperbranched Polyacrylates

Miguel A. D. Gonçalves,[1] *Vigínia D. Pinto,*[1] *Rolando C. S. Dias,**[1] *Mário Rui P. F. N. Costa*[2]

Summary: This work reports the synthesis at 1 L scale of hyperbranched polyacrylates based upon acrylate/diacrylate monomers such as *n*-butyl acrylate (*n*BA)/1,6-hexanediol diacrylate (HDDA) and using atom transfer radical polymerization (ATRP). A FTIR-ATR immersion probe was used to monitor the polymerization reaction. The dynamics of the build-up of polymer structure was studied by off-line analysis of samples at different reaction times by size exclusion chromatography (SEC) with detection of refractive index (RI) and multi-angle laser light scattering (MALLS) signals, leading to molecular weight distribution and *z*-average radius of gyration. Kinetic measurements and observed parameters of the molecular architecture are compared with theoretical predictions which can be used to design new synthesis strategies to improve the homogeneity of hyperbranched polymers. Another goal of this study was elucidating the impact on polymerization of secondary reactions such as intramolecular cyclizations. For comparison purposes, FRP (conventional radical polymerization) of the same monomers is also considered.

Keywords: ATRP; branching; crosslinking; FTIR-ATR; hyperbranched; modeling

Introduction

The design of new advanced materials is a research activity nowadays attracting many scientists and engineers. Stimuli responsive polymers (the so called *smart polymers*) are important examples of advanced materials of microscopic properties changed by variations in external temperature, pH, ionic strength or electromagnetic radiation.

Water compatible smart polymers have important applications in biomedicine bionanotechnology or controlled drug delivery. Insoluble superabsorbent materials exhibiting huge swelling ratios with applications in sanitary industries or separation processes can be obtained from the gelation of multifunctional vinyl monomers. Styrene/divinylbenzene and diacrylic/triacrylic gels are examples of such materials with applications in different domains. Hyperbranched polymers are high molecular mass soluble non-linear tree-like polymers usually presenting useful mechanical properties with reduced melt and solution viscosities. These materials are easier to process than their linear counterparts, being for that reason a subject with intense research activity.

A common feature of microgels (very high molecular mass soluble non-linear polymers), gels or hyperbranched polymers is that their synthesis involve the polymerization of multifunctional monomers, often multivinyl monomers. It is known that classical radical polymerization (FRP) of multifunctional monomers leads to inhomogeneous products due to the relatively slow initiation process as compared to the

[1] LSRE-Instituto Politécnico de Bragança, Quinta de Santa Apolónia, 5300 Bragança, Portugal
Fax: (+351)273313051;
E-mail: mrcosta@fe.up.pt
[2] LSRE-Faculdade de Engenharia da Universidade do Porto, Rua Roberto Frias s/n, 4200-465 Porto, Portugal
Fax: (+351)225081666; E-mail: mrcosta@fe.up.pt

much faster propagation and the occurrence of termination reactions. Formation of loops due to intramolecular cyclization reactions is another mechanism with negative impact in the properties of FRP synthesized non-linear polymers.[1] In the last few years, controlled radical polymerization (CRP) has been tested with the purpose of synthesize hyperbranched/network polymers with improved homogeneity and therefore to obtain products with higher performances in their end-use applications. The use of Atom Transfer Radical Polymerization (ATRP) to obtain acrylate/diacrylate copolymers is an example of such efforts.[2,3]

This work reports experimental and theoretical studies concerning the crosslinking copolymerization of vinyl/divinyl monomers using acrylate/diacrylate chemical systems as case studies. Hyperbranched polyacrylates (only soluble polymers will be here discussed) were synthesized in a laboratory batch reactor and the products were characterized by size exclusion chromatography with detection of refractive index and multi-angle laser light scattering (SEC/RI/MALLS) signals. Chemical properties describing the molecular architecture of these materials were measured, namely molecular weights and *z*-average radius of gyration. The influence of the synthesis technique (ATRP *versus* FRP) on the structure of these materials was also investigated. The FTIR-ATR *in-line* monitoring of these non-linear copolymerizations was also performed in order to assess the ability of this technique to provide information about specific features of the formation mechanisms and structure of hyperbranched polyacrylates (e.g. reactivity of pendent double bonds and cyclizations). FTIR-ATR *in-line* monitoring also has an important potential use for the specification of feed programs with semi-batch reactors which have impact on the molecular architecture of the produced hyperbranched polymers, as recently shown for the system styrene/divinylbenzene.[4]

Kinetic modeling of acrylate/diacrylate copolymerization is a challenging task due to the several mechanisms of branching and crosslinking that must be included in these studies. Here, is shown that a general kinetic approach[5–15] allowing the prediction of molecular weight distributions, sequence length distributions and *z*-average radius of gyration can accommodate these complexities and be exploited to describe some important features of the molecular architecture of hyperbranched polyacrylates. This simulation tool can be useful for carrying out kinetic studies concerning the branching and crosslinking mechanisms and also for the molecular engineering of these materials namely the specification of initial composition, choice of initiator and/or temperature and the design of feeding programs in semi-batch reactor.

Experimental Part

Figure 1 depicts the experimental set-up used in the acrylate/diacrylate crosslinking copolymerizations with *in-line* FTIR-ATR monitoring. Experiments were carried out at 1 L scale. In ATRP experiments, Cu(I)Br of 98% purity, ethyl 2-bromopropionate (EBrP) of 99% purity, *N,N,N′,N″,N‴*-pentamethyldiethylenetriamine (PMDETA) of 99% purity, *n*-butyl acrylate (*n*BA) of 99% purity stabilized with 10 to 55 ppm monomethyl ether hydroquinone (MEHQ), methyl acrylate (MA) of 99% purity stabilized with 100 ppm MEHQ, 1,4-butanediol diacrylate (BDDA) of 90% purity stabilized with 75 ppm hydroquinone, 1,6-hexanediol diacrylate (HDDA) of 80% purity stabilized with 100 ppm MEHQ, bisphenol A ethoxylate diacrylate (BEDA) with $\overline{M}_n \simeq 688$ of 99% purity stabilized with 250 ppm MEHQ, *N,N*-dimethylformamide (DMF) of 99.8% purity were purchased from Sigma Aldrich and used as received. In FRP experiments the same monomers and crosslinkers were used and AIBN of 98% purity and toluene of 99.7% were also purchased from Sigma Aldrich and used as received. Monomers were used as received to mimic the industrial practice. In ATRP experiments, DMF, acrylate

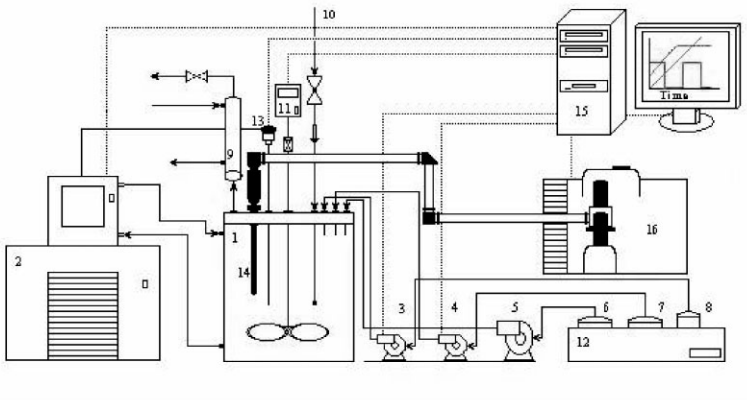

1 – Reaction Vessel (2.5 L)	2 – Thermostatic Bath	3,4 – Peristaltic Pumps
5 – Manual Pump	6,7 – Reservoirs (1 L)	8 – Reservoir (200 mL)
9 – Condenser	10 – Argon Inlet	11 – Mechanical Stirrer
12 – Heating Bath	13 - Thermocouple	14 – ATR Immersion Probe
15 – Computer	16 - FTIR instrument with MCT detector	

Figure 1.
Experimental set-up used in the acrylate/diacrylate crosslinking copolymerizations with *in-line* FTIR-ATR monitoring.

monomer, diacrylate monomer, PMDETA and CuBr were premixed at 60 °C for at least 30 min in a volumetric flask. Good solubility of CuBr in the polymerization system was observed. That mixture was afterwards charged to the reactor, which had previously been purged with argon at a flow rate of 40 mL/min, and brought up to the polymerization temperature (60 °C). When the temperature set-point was attained, the bubbling process was kept for one hour before initiation (as well as for the whole polymerization). Then, the initiator (EBrP) was added to the system defining $t = 0$. At prescribed polymerization times, samples of polymer were withdrawn from the reactor and analyzed by SEC/RI/MALLS. Similar procedures were used in FRP experiments with the exception of the pre-mixing period which is not needed. In different ATRP experiments, the mole fraction of diacrylate in the monomers mixture (y_C) was changed between 0 and 16.8%. Different FRP experiments were performed changing y_C between 0 and 4.1%. A detailed description of these experiments has been presented elsewhere[5] and will not be here reproduced by conciseness.

Molecular weights and average molecular radius of gyration in THF were measured with a Polymer Laboratories PL-GPC-50 integrated SEC system with differential refractometer working at 950 ± 30 nm attached to a Wyatt Technology DAWN8$^+$ HELEOS 658 nm Multi Angle Laser Light Scattering (MALLS) detector. The polymer samples were fractionated by molecular size using a train of 3 GPC columns PL gel (300×7.5 mm) with nominal particle size 10 μm and pore type MIXED-B-LS, maintained at a constant temperature of 30 °C and using THF as the eluent at at flowrate of 1 mL/min. A Wyatt Technology OPTILAB DSP 633 nm interferometric refractometer was used to measure the refractive index increment (dn/dc) for the polymers, solvents and monomers in THF, required for analyzing the MALLS results and for estimating the conversion from the values of the differential refractometer (RI) peak areas of monomers and polymer in the chromatographic traces of the SEC analysis. The

accuracy of this method has been confirmed by gravimetry.

An Axiom Analytical Attenuated Total Reflection (ATR) immersion probe, model DRR207, with ZnSe element, spectral cutoff at 600 cm^{-1}, maximum pressure and temperature operation 60 bar and 280 °C, was used to carry out the *in-line* monitoring of the polymerization reactions. A three arms light guide connects the immersion probe to an ABB Bomem Fourier Transform Infra-Red (FTIR) spectrophotometer, model FTLA2000-104. The spectrophotometer is equipped with an ABB Bomem, Mercury-Cadmium Telluride (MCT) detector (model D10B) which is cooled with liquid nitrogen. The optical system is continuously flushed with argon. Most of ATR-FTIR measurements were performed using the spectrum of air taken at room temperature as the reference background. The use of backgrounds other than air was also tested in this work. The spectra were taken over the full MIR range from 600 cm^{-1} to 4000 cm^{-1} with resolution of 4 cm^{-1}. Each spectrum was calculated from 64 or 128 interferograms.

Mathematical Modeling Including Branching and Crosslinking

It is known[16] that acrylate monomers (among others) are susceptible to undergo chain transfer to monomer reactions because they contain aliphatic tertiary hydrogens which can be involved in a H-atom abstraction, as presented in Figure 2. A new polymer chain created by the resulting radical will contain an unsaturated end group (terminal double bond) capable of undergoing a further reaction with concomitant formation of non-linear structures via Long Chain Branching (LCB). Other sources of LCB in acrylates polymerization are intermolecular chain transfer to polymer mechanisms. These reactions usually involve the H-atom abstraction of a methine group (−CH(R)−) with formation of a mid-chain radical as presented in Figure 3 and/or the H-atom abstraction in a $-CH_3$ group, as depicted in Figure 4. Intermolecular chain transfer to polymer centers (−CH(R)− and $-CH_3$) are created via the incorporation of monomer units in polymer chains (propagation reactions). LCB in acrylates via intermolecular chain transfer to polymer is usually considered to be result of H-atom abstraction of a methine group (Figure 3). For the sake of generality, here both mechanisms will be considered. Termination by combination and termination by disproportionation are also a source of chain transfer to polymer centers (methine groups) and terminal double bonds, respectively. This means that termination mechanisms can also have an indirect contribution for LCB. NMR spectroscopy has been applied to quantify the incidence of the different long chain branching mechanisms[17,18] in different polymerization systems, namely involving *n*BA and vinyl acetate. Gelation due to simultaneous intermolecular chain transfer to polymer and termination by combination was also experimentally observed and theoretically studied in a several works, namely concerning emulsion polymerization of *n*BA.[19–23] The importance of intermolecular chain transfer to polymer was also recently shown through the synthesis of Z-RAFT star acrylate polymers.[24]

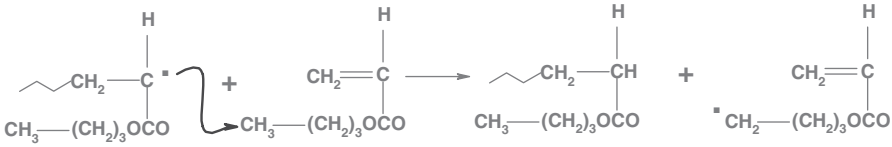

Figure 2.
Depiction of a chain transfer reaction involving an acrylate monomer (*n*-butyl acrylate used for illustration) with creation of a terminal double bond that can lead to long chain branching.

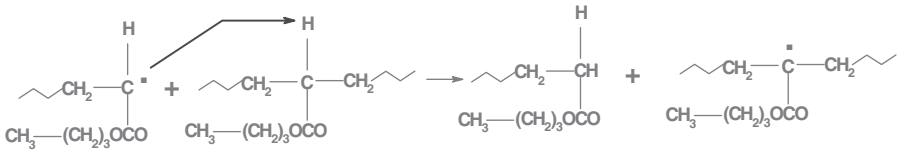

Figure 3.
Depiction of intermolecular chain transfer to polymer in acrylates due to the H-atom abstraction of a methine hydrogen.

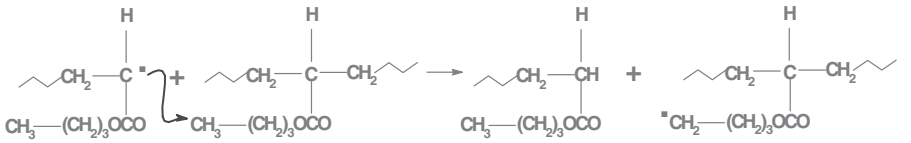

Figure 4.
Depiction of intermolecular chain transfer to polymer in acrylates due to the H-atom abstraction in a $-CH_3$ group.

Intramolecular chain transfer to polymer (backbiting) is also an important source of short chain branching (SCB) in acrylates polymerization. It has been studied in several recent works, namely by Nikitin, Hutchinson and co-workers[25,26,28] aiming to obtain kinetic data and theoretical models of this phenomenon.[20,27,29–32] This mechanism involves the formation of a midchain radical due to the intramolecular abstraction of an H-atom from a neighbor methine group. Additional propagation of this radical leads to the occurrence of SCB in the main polymer chain. These midchain radicals can also undergo β-scission reactions which either reform terminal radicals belonging to short polymer chains or generate terminal double bonds later producing LCB. Propagation, termination and chain transfer reactions involving these species were theoretically and experimentally analyzed and evidence for branching in *n*BA polymerization up to high conversions, due to intramolecular chain transfer to polymer, were thus obtained.[28] Nowadays it is consensual in the scientific community that midchain radicals formed in acrylates polymerization strongly differ from terminal radicals, namely due to their slow propagation rate. A more complex kinetics is therefore expected with polymerization conditions where these effects are dominant. As detailed elsewhere,[5] and also briefly discussed below, it is plausible that intramolecular chain transfer to polymer can be neglected under the experimental conditions (rather low temperature) considered in the present research and therefore this mechanism was not included in our modeling studies.

Besides LCB, non-linear structures are formed in acrylate/diacrylate copolymerization due to the polymerization of pendent double bonds, as depicted in Figure 5. This crosslinking process is intentionally promoted through the addition of the diacrylate monomer to the polymerization system. The amount of divinyl monomer is used in practice to manipulate the extent of the crosslinking process. Reactivity of pendent double bonds and/or incidence of intramolecular cyclization reactions are parameters with a strong influence in the efficiency of crosslinking polymerizations.

In Table 1 is presented the set of chemical groups considered in the mathematical modeling of the ATRP of acrylate/diacrylate monomers performed in the framework of the general kinetic analysis of non-linear irreversible polymerizations previously developed by the authors.[6–15] Nine different kinds of growing radicals are

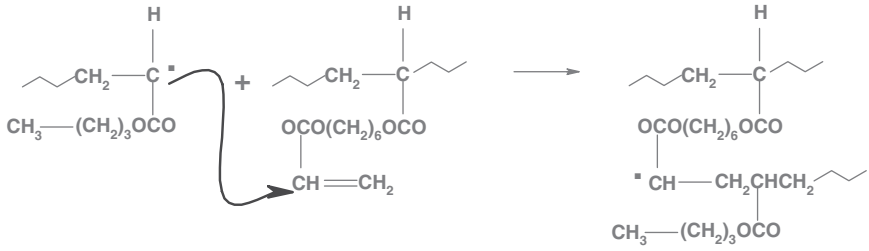

Figure 5.
Depiction of pendent double bonds propagation (crosslinking) in acrylate/diacrylate copolymerization.

Table 1.
Description of the chemical groups considered in the modeling studies of the ATRP copolymerization of acrylate/diacrylate monomers.

Group number	Group description	Alias
1	Growing radical from acrylate monomer	R_1
2	Growing radical from diacrylate monomer	R_2
3	Growing radical from PDB	R_3
4	Growing radical from TDBM	R_4
5	Growing radical from TDBD	R_5
6	Growing radical from HTP	R_6
7	Growing radical from CTP	R_7
8	Growing radical from transfer to acrylate monomer (TAM) reaction	R_8
9	Growing radical from transfer to diacrylate monomer (TDM) reaction	R_9
10	Dormant radical from acrylate monomer	D_1
11	Dormant radical from diacrylate monomer	D_2
12	Dormant radical from PDB	D_3
13	Dormant radical from TDBM	D_4
14	Dormant radical from TDBD	D_5
15	Dormant radical from HTP	D_6
16	Dormant radical from CTP	D_7
17	Dormant radical from transfer to acrylate monomer (TAM) reaction	D_8
18	Dormant radical from transfer to diacrylate monomer (TDM) reaction	D_9
19	Pendant double bond (PDB)	M_3
20	Terminal double bond from transfer to monomer (TDBM)	M_4
21	Terminal double bond from termination by disproportionation (TDBD)	M_5
22	H transfer to polymer center (HTP)	M_6
23	CH_3 transfer to polymer center (CTP)	M_7
24	Acrylate monomer	M_1
25	Diacrylate monomer	M_2
26	Initiator (EBrP)	RX (D_{10})
27	Transition metal/ligand complex (CuBr/PMDETA)	C
28	Deactivator ($CuBr_2$/PMDETA)	CX
29	Radical from initiator	R (R_{10})
30	Solvent	T
31	Primary radical from solvent	R_{11}
32	Dormant primary radical from solvent	D_{11}
33	Polymerized acrylate monomer unit	U_1
34	Polymerized diacrylate monomer unit	U_2
35	Fragment from initiator	F_1
36	Fragment from solvent	F_2
37	Crosslinking site	CS
38	Branching site	BS
39	Non reactive saturated group	SG
40	Internal double bond	IDB

considered (R_1 to R_9) and the correspondent nine different kinds of dormant radicals (D_1 to D_9) are also distinguished due to the ATRP dynamic equilibrium of activation/deactivation. Seven kinds of monomers (M_1 to M_7) are considered: two real monomers (acrylate/diacrylate monomers) and five macromonomers correspondent to pendent double bonds, two kinds of terminal double bonds and also two kinds of intermolecular chain transfer to polymer centers. All these chemical groups (indices from 1 to 23) are reactive and belong to polymer chains. The most general situation with these groups having different reactivities is here considered. Groups with indices 24 to 32 are also reactive but do not belong to polymer chains. This sub-set includes the reactants charged to reactor, namely the two monomers (M_1 and M_2), initiator (RX), transition metal/ligand complex (C) and solvent (T). Other species such as the deactivator (CX) and different kinds of primary active/dormant radicals (R_{10}, R_{11} and D_{11}) are formed/consumed during the polymerization. Groups with indices in the sub-set 33 to 40 belong to polymer chains but are inactive. These chemical groups are needed for the calculation of structural properties of the polymer such as MWD, radius of gyration or crosslinking/branching densities.

Modeling studies here performed considered that these chemical groups are involved in a kinetic scheme with 196 chemical reactions including the following generic mechanisms: reversible activation/deactivation of radicals, initiations, propagations, intermolecular chain transfers to polymer, chain transfers to monomers and solvent, radical terminations by combination and disproportionation. This particular kinetic scheme was discussed elsewhere with some detail[5] and will not be here presented to keep this work within a manageable size. The detailed application of this general kinetic approach to the modeling of other polymerization systems, namely FRP of STY/DVB and MMA/EGDMA, NMRP of STY/DVB and ATRP of MMA/EGDMA was also recently presented.[4,33,34]

Note that even if it is desirable that as many as possible of these kinetic parameters can be measured from experimental data, or indirectly estimated by more or less fundamental models of chemical reactions (an area which is expected to yield more and more accurate predictions in the not so distant future), only a few of them need be accurately known for the range of initial compositions and temperatures in our experiments and the actual number of fitted parameters is very small as discussed in the next section.

The present modeling approach is able to accommodate mechanisms such as intramolecular chain transfer to polymer (backbiting) leading to SCB. Much more complex kinetic schemes must be considered in these circumstances, as previously shown for a case study including primary cyclizations.[11] Results of the present work show that, under the polymerization conditions here considered (diluted solution polymerization at relatively low monomer conversion), crosslinking is dominant relatively to intermolecular chain transfer to polymer leading to LCB and that this mechanism can be neglected in the formation of non-linear architectures. Moreover, is known that SCB is unable to lead to gelation, in contrast to LCB at some particular conditions. The impact of SCB in the development of hyperbranched polyacrylates is even lower than that of LCB and therefore will be not considered in the present analysis.

Chain-length dependence of propagation and termination are important effects in several radical polymerization systems. A recent analysis of these issues[35] conclude that chain-length dependence of propagation can not be neglected in living systems with low average degree of polymerization (e.g. < 10) and that it should also be considered in conventional radical polymerizations with average degree of polymerization lower than 100. It was pointed out that this effect should be negligible for higher values of DP_n.[35]

Scaling laws reflecting the decrease of termination coefficient with DP_n were also presented in recent works.[35,36] These issues are probably even more complex in non-linear radical systems such as those considered in the present work. Due to the high values of DP_n involved in most polymerizations here considered, it is plausible that chain-length dependence of propagation can be neglected. The opposite can be anticipated for the change of termination coefficient with chain length but, as far is of our knowledge, there is no published development of this theory to non-linear radical systems. The general kinetic modeling approach here used is able to deal with chain-length dependence of propagation and termination. However, the need for estimating the full CLD and not simply its moments will increase the associated computing time by 2 or 3 powers of ten.

In-Line FTIR-ATR Monitoring

FTIR-ATR real-time monitoring of vinyl monomers polymerization was reported more than one decade ago.[37,38] In more recent years, further research works were performed with the goal of studying the potentialities of this technique in the solution homo-, co- and terpolymerization of different monomers.[39–41] Owing to its industrial importance, *in-line* FTIR-ATR monitoring of emulsion/miniemulsion polymerization processes is also a subject with growing research activity.[42–45] Indeed, *in-line* FTIR-ATR spectroscopy is a suitable technique to monitor vinyl polymerizations because several difficulties associated with alternative techniques are eliminated: negligible time lags and absence of sampling difficulties are important issues allowing the use of *in-line* FTIR-ATR monitoring to implement feedback control policies. Production of more homogeneous materials is therefore possible using for instance semi-batch reactors. Use in kinetic studies (e.g. quantification of copolymer reactivity ratios) is another important application of this technique. One goal of the present work was the assessment of *in-line* FTIR-ATR spectroscopy in the monitoring of vinyl/divinyl copolymerizations using acrylate/diacrylate model chemical systems. *In-line* FTIR-ATR simultaneous monitoring of vinyl and divinyl monomers can be used to the real time specification of feed policies in semi-batch reactor, which is a possible strategy to design non-linear polymers with tailored properties as recently shown with the system styrene/divinylbenzene.[4]

The spectrum of the various components has enough differences so as to allow their simultaneous quantitative estimation. Figure 6(a) shows the *off-line* FTIR-ATR spectra observed for some monomers used in this work, namely *n*BA, HDDA and BEDA. Vibrational assignments of these acrylate monomers are confirmed and different characteristic absorbance bands can (in principle) be used for the quantitative analysis of these polymerization processes, namely $=CH_2$ twist at $810.6\,cm^{-1}$ and $=CH_2$ deformation at $1409\,cm^{-1}$.[39,40] Note that additional vibrational assignments are identified for BEDA due to the presence of aromatic rings in the chemical structure. In Figure 6(b) are presented the FTIR-ATR spectra observed when *in-line* monitoring the *n*BA homopolymerization with $V_M = 35\%$ confirming the usefulness of this technique to carry out the real-time monitoring of the formation of vinyl polymers.

Nevertheless, real-time monitoring of vinyl/divinyl copolymerization is a challenging task because diluted solution polymerization is required in order to avoid the auto-acceleration effect as non-isothermal temperature profiles make very difficult the quantitative analysis. Moreover, when producing hyperbranched polymers, a low content of divinyl monomer should be used to avoid gelation. Consequently, the intensity of the characteristic bands of divinyl monomer is very low in these copolymerizations; the consequence is a low sensitivity in the monitoring of this component.

It is therefore not unexpected that difficulties arise when the formation of

hyperbranched acrylate/diacrylate copolymers is monitored, as presented in Figure 6(c) for the *n*BA/HDDA copolymerization with $V_M = 35\%$ and $y_C = 0.5\%$: with these operational conditions, the specific sensitivity to the presence of cross-linker is too low, thus precluding the quantitative analysis of important parameters such as the reactivity of pendent double bonds or the formation of intramolecular cyclizations. Similar conclusions are obtained by observation of the spectra in the region 3400 to 4000 cm^{-1} where the polymer formation is detected due to the creation of aliphatic C–H bonds, as represented in Figures 6(d) and 6(e) for the FTIR-ATR monitoring of *n*BA and *n*BA/HDDA copolymerizations, respectively.

Figure 6(f) shows the FTIR-ATR spectra obtained in the *in-line* monitoring of the MA homopolymerization ($V_M = 40\%$) but using the reference background of the initial mixture. In this case, only the polymer formation is also monitored. Notice that the use of reference backgrounds other than the air can be useful in water polymerization media (suspension/emulsion) or when trying to monitor small amounts of divinyl monomers. Indeed, the results here presented show that in the solution production of hyperbranched

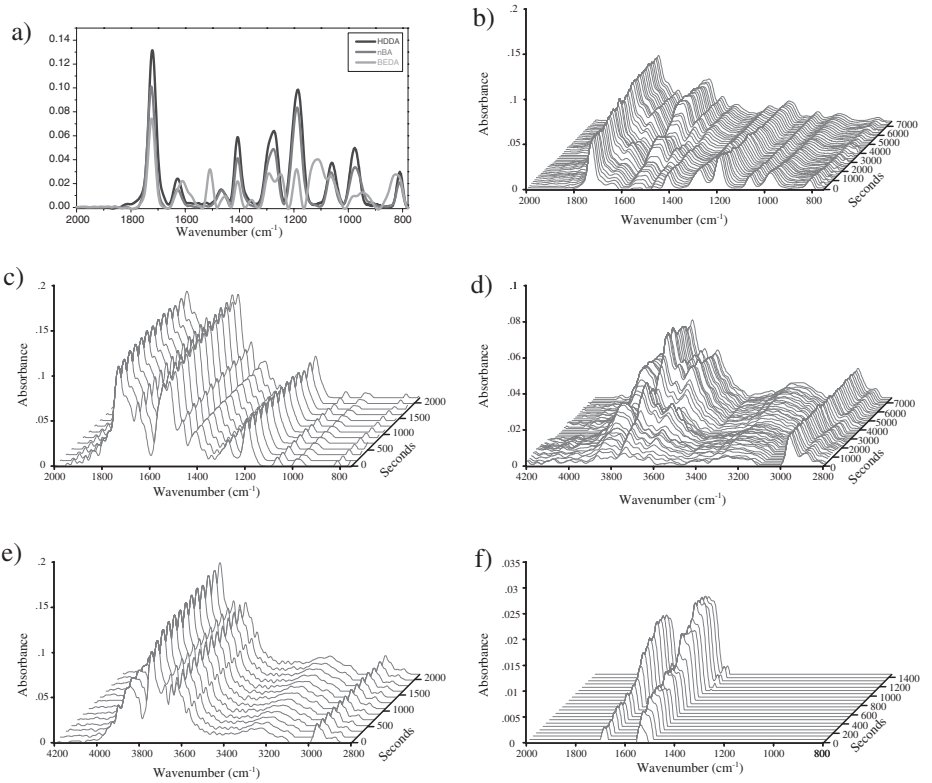

Figure 6.

(a) *Off-line* FTIR-ATR spectra observed for *n*BA, HDDA and BEDA monomers. (b) FTIR-ATR spectra observed in the *in-line* monitoring of the *n*BA homopolymerization with $V_M = 35\%$. (c) FTIR-ATR spectra observed in the *in-line* monitoring of the *n*BA/HDDA copolymerization with $V_M = 35\%$ and $y_C = 0.5\%$. (d) Polymer formation (*n*BA homopolymerization with $V_M = 35\%$) detected by FTIR-ATR monitoring of the region with wave numbers in the range 3400 to 4000 cm^{-1} (aliphatic C-H bonds). (e) Similar analysis as in (d) for *n*BA/HDDA copolymerization with $V_M = 35\%$ and $y_C = 0.5\%$. (f) FTIR-ATR *in-line* monitoring of the MA homopolymerization ($V_M = 40\%$) using the reference background of the initial mixture.

polymers resulting from vinyl/divinyl copolymerization only the vinyl monomer can be *in-line* monitored with reliability.

However, suspension polymerization is a promising way to overcome these difficulties. It should allow work at higher monomer concentrations and extend the polymerization beyond gelation if desired. Higher monomer conversions should also be easier to observe in suspension polymerization therefore yielding higher variations of the intensity of characteristic absorbance bands. These improvements should go in parallel with developments of suspension ATRP which is nowadays a less explored subject than solution ATRP.

Kinetic Modeling of Acrylate/Diacrylate Copolymerization

The general mathematical tool above described and experimental results obtained through the characterization by SEC/RI/MALLS of samples of the produced polymers are here used to carry out the kinetic modeling of acrylate/diacrylate copolymerization. The fast task will be the isolation of the most influential kinetic parameters in the branching and crosslinking processes. The effect of dilution will also be put into evidence and a brief comparison between FRP and ATRP of acrylate/diacrylate monomers is also presented.

Figure 7(a) shows the predicted influence of intermolecular chain transfer to polymer on $\overline{M}_w$ for the solution FRP of *n*BA at $T = 60\,^{\circ}\mathrm{C}$, $V_M = 35\%$, $[I]_0/[M]_0 = 0.1\%$ and $y_C = 0\%$ (without crosslinker). In these simulations, a basic set of kinetic parameters presented in Table 2 was considered[5] and the magnitude of intermolecular chain transfer to polymer was changed through the parameter $C_P = C_{fpH} = 10 \times C_{fpCH3}$. Other parameters were fixed in the simulations, namely those related to polymerization of terminal double bonds ($C_{TDB} = C_{TDBM} = C_{TDBD} = 0$), reactivity of internal polymer radicals ($R_{INT} = 10^{-2}$), reactivity of radicals derived from chain transfer to monomer ($R_{AM} = 1$) and fraction of termination by disproportionation ($\alpha_{td} = 5\%$). Simulations are compared with experimental observations for $\overline{M}_w$ obtained in the solution (toluene) polymerization of *n*BA in the same operation conditions. These results are consistent with a reactivity ratio for intermolecular chain transfer to polymer at maximum of the order of $C_P = 10^{-4}$. Gelation (not observed) is predicted only for much higher values of C_P (e.g. 10^{-3}). Note that chain transfer to solvent is a very important competitive mechanism with chain transfer to polymer which explains the modest incidence of the latter in diluted solution.

Figure 7(b) shows the predicted effect (through changes in the parameter C_{TDBM}) on $\overline{M}_w$ of the polymerization of terminal double bonds created by chain transfer to monomer. Two initial dilutions were considered ($V_M = 35\%$ and $V_M = 100\%$) and the following remaining parameters were considered: $T = 60\,^{\circ}\mathrm{C}$, $[I]_0/[M]_0 = 0.1\%$, $y_C = 0\%$ and $C_P = C_{fpH} = C_{fpCH3} = 0$, $C_{TDBD} = 1$, $R_{INT} = 10^{-2}$, $R_{AM} = 1$, $\alpha_{td} = 5\%$. Hence, this comparison confirms the almost negligible effect of LCB, now via polymerization of terminal double bonds, at higher dilutions. LCB should be more important at nearly bulk polymerization and/or very high monomer conversions.

The predicted influence of intermolecular chain transfer to polymer on $\overline{M}_w$ for the solution ATRP of *n*BA at $T = 60\,^{\circ}\mathrm{C}$, $V_M = 35\%$, M/I/CuBr/PMDETA = 50/1/0.45/0.5 and $y_C = 0\%$ is put into evidence in Figure 7(c). Chain transfer to polymer centers were distinguished ($C_P = C_{fpH} = 10 \times C_{fpH}$) and the following simulation parameters were also considered: $C_{TDB} = C_{TDBM} = C_{TDBD} = 1$, $R_{INT} = 10^{-1}$, $R_{AM} = 1$ and $\alpha_{td} = 5\%$. Comparison with experimental results shows that, for higher dilutions, the influence of LCB in ATRP should also be very low. Note that the incidence of termination reactions, namely termination by combination, is much more pronounced in FRP than in ATRP. Termination by combination plays a special role in LCB development, namely in gel

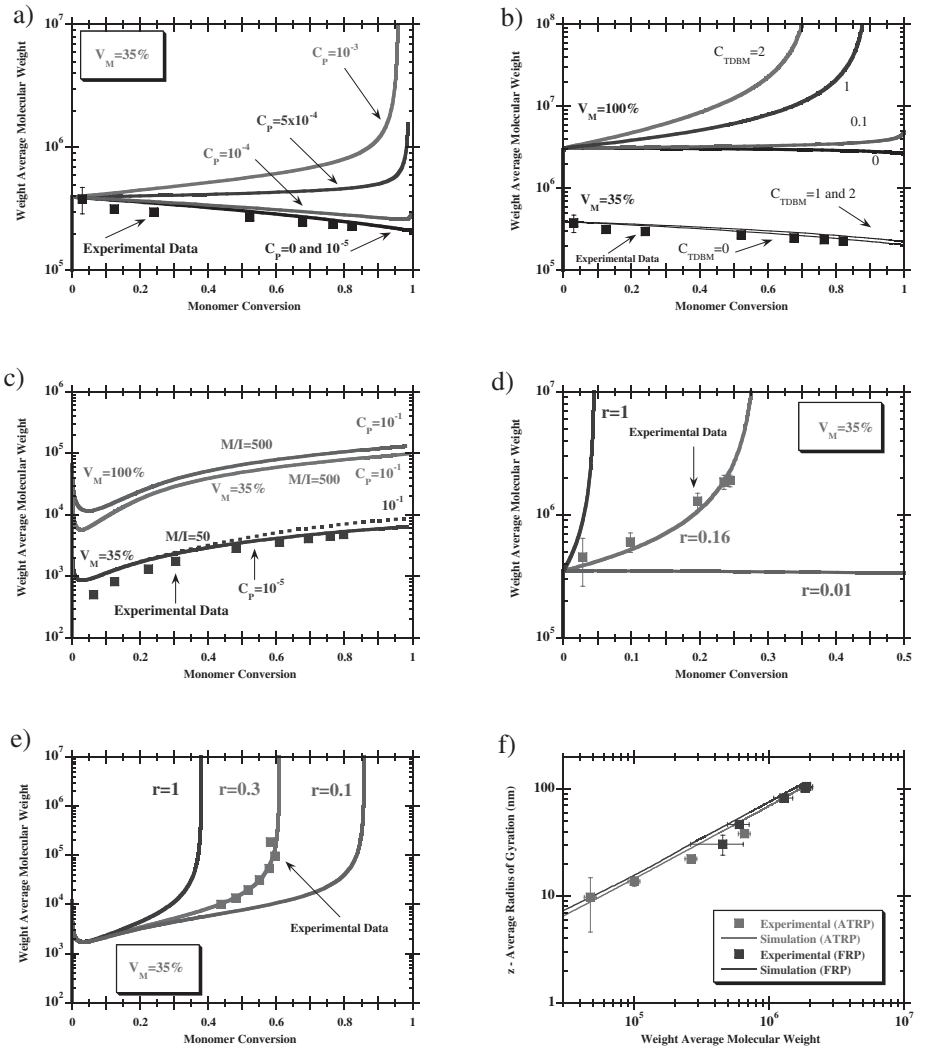

Figure 7.
(a) Predicted influence of intermolecular chain transfer to polymer on $\overline{M}_w$ for the solution ($V_M = 35\%$) FRP of *n*BA. (b) Predicted influence of polymerization of terminal double bonds on $\overline{M}_w$ for FRP of *n*BA at different dilutions. (c) Predicted influence of LCB on $\overline{M}_w$ for the ATRP of *n*BA. (d) Predicted effect of the reactivity of PDB on $\overline{M}_w$ for FRP of *n*BA/HDDA. (e) Predicted effect of the reactivity of PDB on $\overline{M}_w$ for ATRP of *n*BA/HDDA. (f) Relation $\overline{R}_g$ *versus* $\overline{M}_w$ for FRP (*n*BA/HDDA, $y_C = 0.5\%$) and ATRP (*n*BA/BEDA, $y_C = 5\%$, $[M]_0/[I]_0 = 200$) hyperbranched polyacrylates. $T = 60$ C in all simulations.

formation due to this mechanism. Even increasing the primary chain length (increasing the initial ratio $[M]_0/[I]_0$), under the experimental conditions here used, LCB has a tiny contribution for the formation of non-linear structures in ATRP. Figure 7(d) shows the effect of the reactivity of PDB (quantified by the parameter r) on $\overline{M}_w$ for FRP synthesized polyacrylates using $T = 60\,^{\circ}\mathrm{C}$, $V_M = 35\%$, $[I]_0/[M]_0 = 0.1\%$ and $y_C = 0.5\%$. Besides crosslinking, simulations also take into account LCB with help of the following parameters: $C_P = C_{fpH} = C_{fpCH3} = 10^{-4}$, $C_{TDBM} = C_{TDBD} = 1$, $R_{INT} = 10^{-2}$, $R_{AM} = 1$, $\alpha_{td} = 5\%$. It can be noticed the strong

Table 2.
Basic set of rate coefficients considered in the modeling studies of the FRP and ATRP copolymerization of acrylate/diacrylate monomers.

Kinetic step	Rate coefficient expression	Ref.
Initiator thermal decomposition (AIBN)	$k_d = 4.31 \times 10^{15} \exp(-131.7 \times 10^3/RT)$ (s^{-1}), $f = 0.6$	[46]
*n*BA propagation	$k_p = 2.21 \times 10^7 \exp(-17.9 \times 10^3/RT)$	[47]
Chain transfer to monomer (*n*BA)	$k_{fM} = 2.9 \times 10^5 \exp(-32.6 \times 10^3/RT)$	[48]
Chain transfer to solvent	$C_S = k_{fS}/k_p = 2.7 \times 10^{-4}$	[46]
Intermolecular chain transfer to polymer	$10^{-5} < C_P = k_{fp}/k_p < 10^{-3}$	[49],[a]
Radical termination	$k_p/\sqrt{k_t} = 0.15 + 0.4[M]$	[50]
Combination/Disproportionation	$\alpha_{td} = k_{td}/k_t = 0.05$, $\alpha_{tc} = k_{tc}/k_t = 0.95$	[46]
Equilibrium constant (ATRP)	$K_{ATRP}k_a/k_{da} = 3.27 \times 10^{-8}$	[51]
Radical deactivation (ATRP)	$k_{da} = 6.1 \times 10^6$	[52]
Propagation of terminal double bonds	$0.01 \leq C_{TDB} = k_p^{**}/k_p \leq 1$	*a*
Propagation of pendent double bonds	$0.01 \leq r = k_p^{*}/k_p \leq 1$	*a*

[a]This work.
Kinetic parameters expressed in $dm^3\,mol^{-1}\,s^{-1}$, unless otherwise stated.
$R = 8.314\ J\,mol^{-1}\,K^{-1}$.

impact of the reactivity of PDB on the polymer properties, showing that this mechanism is the dominating phenomenon in these kind of polymerization systems. Comparison of experimental results with predictions allows the fitting of this parameter, as shown in Figure 7(d). For this particular case study, $r = 0.16$ is obtained, indicating an apparently much lower reactivity of PDB than acrylate double bonds. It is plausible that this reactivity ratio of PDB is much lower than one mostly owing to the effect of intramolecular cyclizations which had not been considered in the modeling studies. Intramolecular cyclizations consume PDB and consequently decrease the crosslinking efficiency which is also reflected by delaying gelation. These effects are specially important at higher dilution, as more deeply discussed elsewhere[4,5,33,34] for different kinds of polymerization systems.

A similar fitting procedure is presented in Figure 7(e) for ATRP synthesized polyacrylates using $T = 60\,^{\circ}C$, $V_M = 35\%$, M/I/CuBr/PMDETA = 50/1/0.45/0.5, $y_C = 10\%$. LCB was also taken into account in the calculations considering: $C_P = C_{fpH} = C_{fpCH3} = 10^{-4}$, $C_{TDBM} = C_{TDBD} = 1$, $R_{INT} = 10^{-1}$, $R_{AM} = 1$, $\alpha_{td} = 5\%$. Also for ATRP, polymerization of PDB is the major factor governing the crosslinking process and therefore the formation of hyperbranched structures. A higher value for the apparent reactivity of PDB was here obtained ($r = 0.3$) indicating that intramolecular cyclizations are also present in ATRP but with a much lesser extent that in FRP. These results show that ATRP can be used to synthesize hyperbranched polymers with more homogeneous structure than those obtained by FRP and also with a higher level of control. Note also that, comparatively to FRP, a much high level of crosslinker can be used in ATRP without occurrence of gelation.

In Figure 7(f) it is shown the relation $\overline{R}_g$ *versus* $\overline{M}_w$ for FRP (*n*BA/HDDA, $y_C = 0.5\%$) and ATRP (*n*BA/BEDA, $y_C = 5\%$, $[M]_0/[I]_0 = 200$) synthesized hyperbranched polyacrylates. Good agreement between experimental measurements and predictions is observed for both systems, confirming the good predictive power of the theoretical approach[14] used in the simulations despite the remaining uncertainty concerning the magnitude of the expansion factor for branched polymers. Interestingly, with all these branched polymers a nearly identical relation $\overline{R}_g$ *versus* $\overline{M}_w$ is observed despite the expected structural dissimilarities between their formation by FRP and ATRP. For the results presented in Figure 7(f), a scaling law $\overline{R}_g = K_G \overline{M}_w^{\nu}$ is observed and the estimated exponent is $\nu = 0.65$ which deviates from

the value $\nu = 0.5-0.6$ expected for linear random coils. A detailed discussion concerning the relation between radius of gyration and molecular weight involving the present chemical systems can be found elsewhere.[5] Polymer physics of branched/crosslinking polymers is a complex subject with important observed deviations from a power law behavior, as reported recently for branched polysacharides.[53] A more rigorous theory for the prediction of physical properties of non-linear polymers should more correctly calculate the effect of excluded volume expansion and tke into account the presence of intramolecular loops.

The predictive value of the developed kinetic model is hampered by the high number of kinetic parameters to be known. This problem has been often alleviated by performing a sensitivity analysis of the predictions leaving only a restricted set of kinetic parameters to fit. Indeed, for these systems this approach shows that LCB is a minor effect as compared to crosslinking. Other uses of this strategy are illustrated in Figure 8(a) where additional results concerning the sensitivity analysis of the kinetic parameters are shown, namely concerning the influence of the reactivity of the radicals from transfer to monomer. These simulations show that, if the radicals from transfer to monomer are reactive enough, under bulk polymerization, gelation can occur due to LCB originated by chain transfer to monomer. A different combination of kinetic parameters was considered in the simulations presented in Figure 8(b) where the dynamics of crosslinking/branching density (average number of crosslinking/branching sites per polymer molecule) is shown. Here crosslinking and LCB are simultaneously considered and different reactivities are assumed for different kinds of polymer radicals. Note the much higher contribution of crosslinking to the non-linear density, comparatively to LCB.

Distinctive features of the used kinetic approach concerning the prediction of the dynamics of the z-average radius of gyration in Θ state are illustrated in Figure 9. The effect of the reactivity of pendant double bonds and of the initial mole fraction of crosslinker on the time evolution of this physical property is predicted for operation in batch reactor. These predictions can be compared with measurements of $\overline{R}_g$ performed in a good solvent, as presented elsewhere.[5]

The interpretation of SEC/RI/MALLS data of highly branched/crosslinked polymer samples is a particularly difficult task because inversions in the relation molecular mass versus elution volume are possible

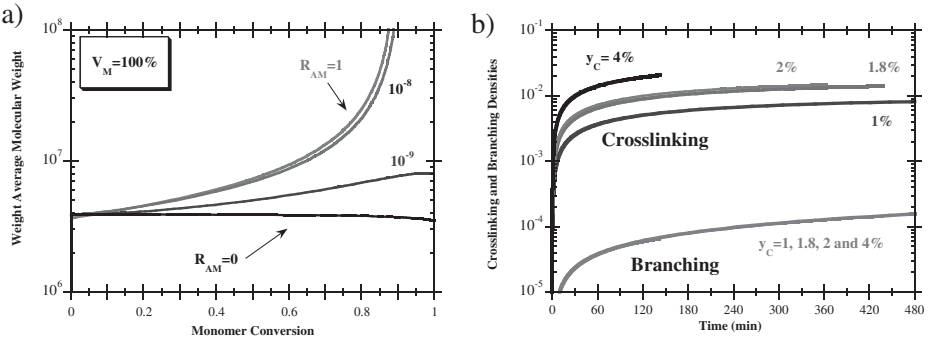

Figure 8.

(a) Predicted effect of the reactivity of radicals from transfer to monomer on $\overline{M}_w$ of FRP synthesized polyacrylates. Operation conditions: $T = 60\ ^\circ C$, $V_M = 100\%$, $[I]_0/[M]_0 = 0.1\%$, $y_C = 0\%$. Kinetic parameters: $C_P = C_{fpH} = C_{fpCH_3} = 0$, $C_{TDBM} = C_{TDBD} = 1$, $R_{INT}\ 10^{-2}$, $\alpha_{td} = 5\%$. (b) Predicted effect of the initial amount of crosslinker on the dynamics of crosslinking and branching densities of ATRP synthesized polyacrylates. Operation conditions: $T = 60\ ^\circ C$, $V_M = 35\%$, M/I/CuBr/PMDETA = 50/1/0.45/0.5. Kinetic parameters: $C_{PDB} = C_{TDBM} = C_{TDBD} = 1$, $C_{fpH} = 10^{-4}$, $C_{fpCH_3} = 10^{-5}$, $R_{PDB} = R_{INT} = 0.1$, $R_{AM} = 1$, $\alpha_{td} = 5\%$.

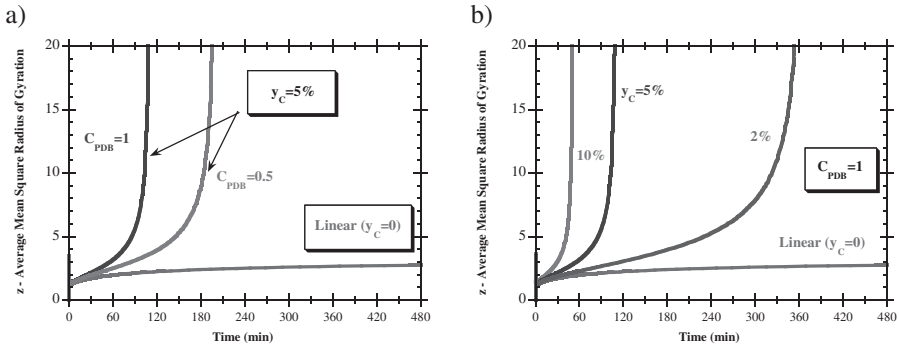

Figure 9.
(a) Predicted effect of the reactivity of pendant double bonds on the dynamics of the *z*-average mean square radius of gyration (Θ state and normalization by the bond length, $\overline{R}_g/b$) of ATRP synthesized polyacrylates. Operation conditions: $T = 60\,^{\circ}C$, $V_M = 35\%$, M/I/CuBr/PMDETA = 50/1/0.45/0.5. Initial mole fraction of crosslinker: $y_C = 5\%$. Kinetic parameters: $C_{TDBM} = C_{TDBD} = 1$, $C_{fpH} = 10^{-4}$, $C_{fpCH_3} = 10^{-5}$, $R_{PDB} = R_{INT} = 0.1$, $R_{AM} = 1$, $\alpha_{td} = 5\%$, $K_{ATRP} = 1.25 \times 10^{-10}$, $C_I = 1$. (b) Predicted effect of the initial mole fraction of crosslinker on the dynamics of the *z*-average mean square radius of gyration of ATRP synthesized polyacrylates (same conditions of (a)).

as reported in some recent works.[34,54] These observations are a consequence of the existence in non-linear polymer of populations with the same molecular weight but very different molecular sizes. Important advances concerning the theory of multiple-detection by SEC of non-linear polymers were recently obtained showing that some current commercial software used in the calculation of average molecular weights are affected by significant errors.[55] A rigorous interpretation of the SEC traces of non-linear should take into account these reported limitations and also the difficulties associated with the existence in these polymer populations of position isomers leading to molecules with the same molecular weight but different molecular size. As far as it is of our knowledge this is an open issue.

In Figure 10(a) are presented the measured refractive index and light scattering

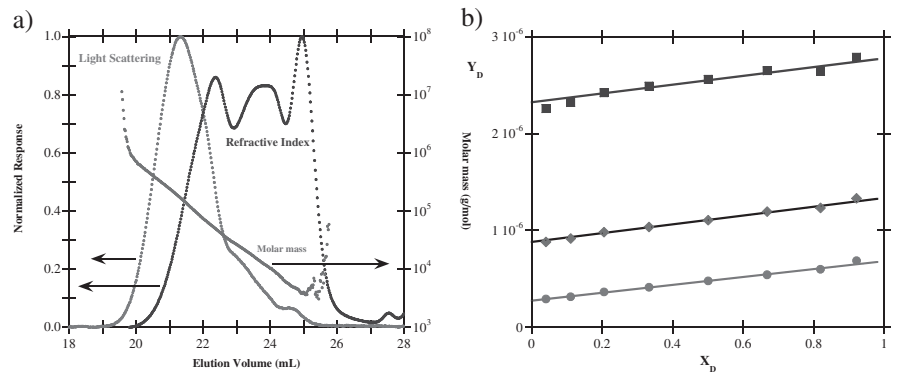

Figure 10.
(a) Measured refractive index and light scattering (90 °) signals in the SEC trace of an ATRP synthesized Acrylate/Diacrylate sample. Change of molecular mass along the elution volume is also showed. (b) Examples of Debye plots along the SEC trace of a branched polyacrylate sample. Three different elution volumes were considered. The measured signals with the eight MALLS detectors are showed.

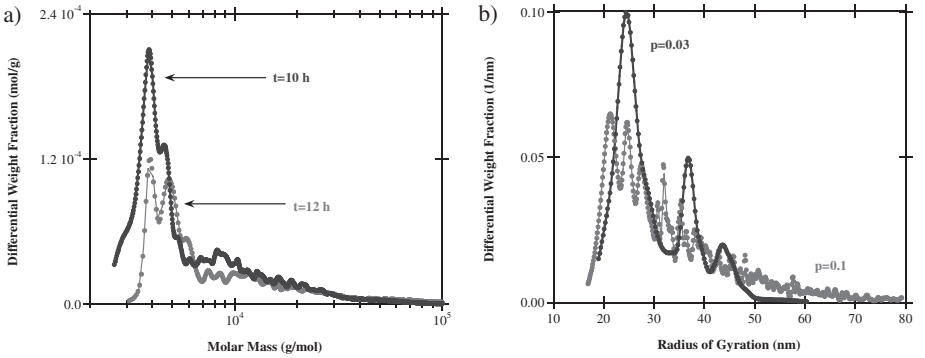

Figure 11.
(a) Typical differential weight fraction of the molar mass distributions measured for branched polyacrylate samples. Time evolution of the crosslinking process can be observed. (b) Typical differential weight fraction of the radius of gyration distributions measured for branched polyacrylate samples. Change of the distribution with monomer conversion is depicted.

(90 °) signals in the SEC trace of an ATRP synthesized Acrylate/Diacrylate sample. The detection by SEC/RI/MALLS of a polymer cluster with high molecular weight but with very low concentration is detected when gelation is approached. In the same figure, the change of the molar mass with the elution volume is also presented. Molar mass and radius of gyration of each slice in a SEC/RI/MALLS system are often calculated using a Debye plot, as exemplified in Figure 10(b) with $X_D = \sin^2(\theta/2)$ and $Y_D = K^*c/R(\theta)$. The intercept with the Y axis yields the molar mass and the slope of the fitted straight line yields the radius of gyration. Using this information and considering that each slice is monodisperse, it is possible to obtain estimates of the differential weight fractions of the molar mass and radius of gyration distributions, as exemplified in Figure 11 for branched polyacrylates. In this case, multimodal distributions seem to occur. Multimodal CLD in controlled living polymerization of vinyl/divinyl monomers were recently predicted using the present kinetic approach.[56]

Conclusion

In this work, hyperbranched polyacrylates were synthesized through the ATRP of acrylate/diacrylate monomers. For comparison purposes, FRP of the same monomers was also performed. Solution polymerization reactions were *in-line* monitored using a FTIR-ATR immersion probe and products were characterized by SEC/RI/MALLS. Dynamics of molecular weights and of z-average radius of gyration were measured in batch reactor.

A general kinetic approach allowing the prediction of important details of the molecular architecture of non-linear polymers was applied to those hyperbranched polyacrylates with crosslinking and branching mechanisms simultaneously considered. Comparison of simulations with experimental results obtained by SEC/RI/MALLS leads to conclude that, under the experimental conditions used in this study, crosslinking is the dominant mechanism in the formation of non-linear architectures and that long chain branching can be neglected. The effect of cyclizations on the molecular architecture of these products was also detected: ATRP allows the production of more homogeneous hyperbranched polyacrylates (less intramolecular cyclizations) than FRP but, even with ATRP, this mechanism becomes increasing important with dilution. It was also shown that, besides molecular weights, the z-average radius of gyration can also be

predicted with reliability in the framework of the present kinetic approach. The good foundations of this simulation tool make it useful to design hyperbranched polymers with tailored properties.

It was concluded that *in-line* FTIR-ATR is a reliable technique to monitor the acrylate monomer in solution acrylate/diacrylate copolymerization but the *in-line* monitoring of diacrylate monomer is a challenging task. The use of diluted polymerization systems with the goal of obtaining isothermal profiles and a low content of diacrylate monomer to avoid gelation are drawbacks for the monitoring of diacrylate monomers by this technique. Improved results are expected with suspension polymerization concerning, not only the production of hyperbranched polymers with a higher homogeneity (minimization of cyclizations), but also better performing the *in-line* monitoring of divinyl monomers. With an operation at a much higher content of divinyl monomer it is possible to keep isothermal profiles and the polymerization can be extended to the post gelation period if desired.

Notation

c	concentration of solute molecules in MALLS.
$C_P = k_{fP}/k_p$	reactivity ratio for global intermolecular chain transfer to polymer.
C_{fpH}	reactivity ratio for intermolecular chain transfer to HTP.
C_{fpCH3}	reactivity ratio for intermolecular chain transfer to CTP.
$C_{TDB} = k^{**}/k_p$	reactivity ratio for global polymerization of terminal double bonds.
C_{TDBM}	reactivity ratio for polymerization of TDBM.
C_{TDBD}	reactivity ratio for polymerization of TDBD.
$C_S = k_{fS}/k_p$	reactivity ratio for chain transfer to solvent.
dn/dc	refractive index increment with respect to the concentration of the polymer solution.
DP_n	number average degree of polymerization.
f	thermal initiator decomposition efficiency.
[I]	initiator concentration (mol/dm^3).
k_a	rate coefficient of radical activation in ATRP.
k_{da}	rate coefficient of radical deactivation in ATRP.
k_d	rate coefficient of the unimolecular thermal initiator decomposition.
k_{fM}	rate coefficient of the chain transfer to monomer.
k_{fP}	rate coefficient of the intermolecular chain transfer to polymer.
k_{fS}	rate coefficient of the chain transfer to solvent.
k_p	rate coefficient of the propagation of vinyl monomer.
k_{pi1}	rate coefficient of the propagation of radical i with vinyl monomer.
k_p^*	rate coefficient of the propagation of pendent double bonds.
k_p^{**}	rate coefficient of the propagation of terminal double bonds.
k_t	rate coefficient of the global radical termination.
k_{tc}	rate coefficient of the radical termination by combination.
k_{td}	rate coefficient of the radical termination by disproportionation.
$K^* = 4\pi^2(dn/dc)^2 n_0^2/(N_A\lambda_0^4)$	parameter in the light scattering equation.
$K_{ATRP} = k_a/k_{da}$	equilibrium constant for radical activation/deactivation (ATRP).

K_G	coefficient in the scaling law $\overline{R}_g$ *versus* $\overline{M}_w$.
$[M]$	monomer concentration (mol/dm^3).
$\overline{M}_n$	number-average relative molecular mass.
$\overline{M}_w$	weight-average relative molecular mass.
$\overline{M}_z$	z-average relative molecular mass.
n_0	refractive index of the solvent in MALLS.
N_A	number of Avogadro.
$r = k_p^*/k_p$	reactivity ratio for the propagation of pendent double bonds.
R	ideal gas constant ($R = 8.314$ Jmol^{-1}K^{-1}).
$R(\theta)$	fraction of light scattered in MALLS, per unit of solid angle, in excess of the light scattered by the solvent, normalized by incident intensity of the light.
$\overline{R}_g$	root z-average mean square radius of gyration.
$R_{AM} = k_{pi1}/k_p$	reactivity ratio for radicals derived from chain transfer to monomer ($i = 8$ and 9 as described in Table 1.)
$R_{INT} = k_{pi1}/k_p$	reactivity ratio for internal radicals ($i = 3, ..., 7$ as described in Table 1.)
t	time.
T	temperature.
V_M	volume fraction of vinyl monomer in the solution.
$X_D = \sin^2(\theta/2)$	X coordinate in a Debye plot.
y_C	mole fraction of divinyl monomer in the monomers mixture.
$Y_D = K^*c/R(\theta)$	Y coordinate in a Debye plot.

Greek Characters

α_{tc}	probability of radical termination by combination.
α_{td}	probability of radical termination by disproportionation.
λ_0	vacuum wavelength of the incident light in MALLS.
ν	exponent in the scaling law $\overline{R}_g$ *versus* $\overline{M}_w$.
θ	scattering angle in MALLS.

Subscripts

n	number average.
w	weight average.
z	z-average.
0	initial.

Abbreviations

AIBN	2,2′-azobis(2-methylpropionitrile).
ATR	Attenuated Total Reflection.
ATRP	Atom Transfer Radical Polymerization.
BDDA	1,4-Butanediol Diacrylate.
BEDA	Bisphenol A Ethoxylate Diacrylate.
BS	Branching site formed due to chain transfer to polymer or polymerization of a terminal double bond.
C	ATRP transition metal (e.g. CuBr).
CLD	chain length distribution.
CX	ATRP oxidized transition metal (e.g. $CuBr_2$).
CRP	Controlled Radical Polymerization.
CS	Crosslinking site formed due to the polymerization of a pendent double bond.
CTP	CH_3 transfer to polymer center.
D_i	Dormant radical of the kind i, as described in Table 1.
DMF	*N,N*-dimethylformamide.
DVB	Divinylbenzene.
EBrP	Ethyl 2-Bromopropionate.
EGDMA	Ethylene Glycol Dimethacrylate.
F_i	Molecular fragment of the kind i, as described in Table 1.
FRP	Free Radical Polymerization (conventional).

FTIR	Fourier Transform Infra-Red.
HDDA	1,6-Hexanediol Diacrylate.
HTP	H transfer to polymer center.
I	Initiator.
IDB	Internal double bond formed due to termination by disproportionation of internal radicals (R_3 to R_7).
LCB	Long Chain Branching.
M	monomer.
M_i	Monomer or macromonomer of the kind i, as described in Table 1.
MA	Methyl Acrylate.
MEHQ	Monomethyl Ether Hydroquinone.
MCT	Mercury-Cadmium-Telluride detector.
MMA	Methyl Methacrylate.
MWD	Molecular Weight Distribution.
*n*BA	*n*-Butyl Acrylate.
NMR	Nuclear Magnetic Resonance.
NMRP	Nitroxide-Mediated Radical Polymerization.
PDB	Pendant Double Bond.
PMDETA	*N,N,N′,N″,N″*-Pentamethyldiethylenetriamine.
R_i	Growing radical of the kind i, as described in Table 1.
RX	ATRP initiator.
RAFT	Reversible Addition-Fragmentation Chain Transfer polymerization.
RG	Root Mean-Square Radius of Gyration.
S	styrene.
SEC/RI/MALLS	Size Exclusion Chromatography with Refractive Index and Multi-Angle Laser Light Scattering detection.
SCB	Short Chain Branching.
SG	Non reactive saturated group (e.g. due to termination by disproportionation).
T	solvent.
TAM	Transfer to Acrylate Monomer reaction.
TDBD	Terminal Double Bond from termination by Disproportionation.
TDBM	Terminal Double Bond from chain transfer to Monomer.
TDM	Transfer to Diacrylate Monomer reaction.
THF	Tetrahydrofuran.
U_i	Polymerized monomer unit of the kind i, as described in Table 1.

Acknowledgements: Financial support by Fundação para a Ciência e a Tecnologia (FCT), Ministry of Science and Technology of Portugal and European Community (FEDER) through project POCI-PPCDT/EQU/60483/2004 is gratefully acknowledged.

[1] A. Matsumoto, *Adv. Polym. Sci.* **1995**, *123*, 41.
[2] H. Gao, K. Min, K. Matyjaszewski, *Macromolecules* **2007**, *40*, 7763.
[3] H. Gao, W. Li, K. Matyjaszewski, *Macromolecules* **2008**, *41*, 2335.
[4] M. A. D. Gonçalves, R. C. S. Dias, M. R. P. F. N. Costa, *Macromol. Symp.* **2007**, *259*, 124.
[5] M. A. D. Gonçalves, R. C. S. Dias, M. R. P. F. N. Costa, *Macromol. Symp.* **2010**, *289*, 1.
[6] M. R. P. F. N. Costa, R. C. S. Dias, *Chem. Eng. Sci.* **1994**, *49*, 491.
[7] M. R. P. F. N. Costa, R. C. S. Dias, *Macromol. Theory Simul.* **2003**, *12*, 560.
[8] R. C. S. Dias, M. R. P. F. N. Costa, *Macromolecules* **2003**, *36*, 8853.
[9] M. R. P. F. N. Costa, R. C. S. Dias, *Chem. Eng. Sci.* **2005**, *60*, 423.
[10] R. C. S. Dias, M. R. P. F. N. Costa, *Macromol. Theory Simul.* **2005**, *14*, 243.
[11] R. C. S. Dias, M. R. P. F. N. Costa, *Polymer* **2005**, *46*, 6163.
[12] R. C. S. Dias, M. R. P. F. N. Costa, *Polymer* **2006**, *47*, 6895.
[13] M. R. P. F. N. Costa, R. C. S. Dias, *Macromol. Symp.* **2006**, *243*, 72.
[14] M. R. P. F. N. Costa, R. C. S. Dias, *Polymer* **2007**, *48*, 1785.
[15] R. C. S. Dias, M. R. P. F. N. Costa, *Macromol. React. Eng.* **2007**, *1*, 440.
[16] R. A. Hutchinson, A. Penlidis, *Polymer Reaction Engineering*, (Chapter 3) **2007**, Blackwell Publishing.
[17] D. Britton, F. Heatley, P. A. Lovell, *Macromolecules* **1998**, *31*, 2828.
[18] N. M. Ahmad, F. Heatley, P. A. Lovell, *Macromolecules* **1998**, *31*, 2822.
[19] G. Arzamendi, J. Forcada, J. M. Asúa, *Macromolecules* **1994**, *27*, 6068.

[20] C. Plessis, G. Arzamendi, J. R. Leiza, H. A. S. Schoonbrood, D. Charmot, J. M. Asúa, *Macromolecules* **2000**, *33*, 5041.
[21] C. Plessis, G. Arzamendi, J. R. Leiza, H. A. S. Schoonbrood, D. Charmot, J. M. Asúa, *Ind. Eng. Chem. Res.* **2001**, *40*, 3883.
[22] I. González, J. R. Leiza, J. M. Asúa, *Macromolecules* **2006**, *39*, 5015.
[23] I. González, J. M. Asúa, J. R. Leiza, *Polymer* **2007**, *48*, 2542.
[24] D. Boschmann, P. Vana, *Macromolecules* **2007**, *40*, 2683.
[25] A. N. Nikitin, R. A. Hutchinson, *Macromolecules* **2005**, *38*, 1581.
[26] A. N. Nikitin, R. A. Hutchinson, *Macromol. Theory Simul.* **2006**, *15*, 128.
[27] A. N. Nikitin, R. A. Hutchinson, M. Buback, P. Hesse, *Macromolecules* **2007**, *40*, 8631.
[28] A. N. Nikitin, R. A. Hutchinson, G. A. Kalfas, J. R. Richards, C. Bruni, *Macromol. Theory Simul.* **2009**, *18*, 247.
[29] W. Wang, R. A. Hutchinson, *Macromol. React. Eng.* **2008**, *2*, 199.
[30] R. X. E. Willemse, A. M. van Herk, E. Panchenko, T. Junkers, M. Buback, *Macromolecules* **2005**, *38*, 5098.
[31] C. Barner-Kowollik, F. Günzler, T. Junkers, *Macromolecules* **2008**, *41*, 8971.
[32] M. Buback, P. Hesse, T. Junkers, T. Sergeeva, T. Theis, *Macromolecules* **2008**, *41*, 288.
[33] I. M. R. Trigo, M. A. D. Gonçalves, R. C. S. Dias, M. R. P. F. N. Costa, *Macromol. Symp.* **2008**, *271*, 107.
[34] M. A. D. Gonçalves, I. M. R. Trigo, R. C. S. Dias, M. R. P. F. N. Costa, *Macromol. Symp.* **2010**, *291–292*, 239.
[35] J. P. A. Heuts, G. T. Russel, G. B. Smith, A. M. van Herk, *Macromol. Symp.* **2007**, *248*, 12.
[36] G. B. Smith, G. T. Russel, *Macromol. Symp.* **2007**, *248*, 1.
[37] E. G. Chatzi, O. Kammona, C. Kiparissides, *J. Appl. Polym. Sci.* **1997**, *63*, 799.
[38] R. F. Storey, A. B. Donnalley, T. L. Maggio, *Macromolecules* **1998**, *31*, 1523.
[39] H. Hua, M. A. Dubé, *J. Polym. Sci. A: Polym Chem* **2001**, *39*, 1860.
[40] R. Jovanović, M. A. Dubé, *J. Appl. Polym. Sci.* **2001**, *82*, 2958.
[41] H. Hua, T. Rivard, M. A. Dubé, *Polymer* **2004**, *45*, 345.
[42] S. Roberge, M. A. Dubé, *J. Appl. Polym. Sci.* **2007**, *103*, 46.
[43] H. Hua, M. A. Dubé, *Polymer Reaction Engineering* **2002**, *10*, 21.
[44] K. Ouzineb, H. Hua, R. Jovanović, M. A. Dubé, T. F. McKenna, *C. R. Chimie* **2003**, *6*, 1343.
[45] R. Jovanović, M. A. Dubé, *Polymer Reaction Engineering* **2003**, *11*, 233.
[46] G. Moad, D. H. Solomon, *The Chemistry of Radical Polymerization* **2006**, 2nd Ed., Elsevier, Oxford
[47] J. M. Asúa, S. Beuermann, M. Bubak, P. Castignolles, B. Charleux, R. G. Gilbert, R. A. Hutchinson, J. R. Leiza, A. N. Nikitin, J.-P. Vairon, A. M. van Herk, *Macromol. Chem. Phys.* **2004**, *205*, 2151.
[48] S. Maeder, R. G. Gilbert, *Macromolecules* **1998**, *31*, 4410.
[49] J. Brandrup, E. H. Immergut, E. A. Grulke, *Polymer Handbook*, **1999**, 4th Ed., John Wiley & Sons, New York
[50] T. F. McKenna, A. Villanueva, A. M. Santos, *J. Polym. Sci. Part A: Polym. Chem.* **1999**, *37*, 571.
[51] W. Tang, N. V. Tsarevsky, K. Matyjaszewski, *J. Am. Chem. Soc.* **2006**, 1598.
[52] K. Matyjaszewski, H.-J. Paik, P. Zhou, S. J. Diamantini, *Macromolecules* **2001**, *34*, 5125.
[53] A. Rolland-Sabaté, M. G. Mendez-Montealvo, P. Colonna, V. Planchot, *Biomacromolecules* **2008**, *9*, 1719.
[54] I. Bannister, N. C. Billingham, S. P. Armes, S. P. Rannard, P. Findlay, *Macromolecules* **2006**, *39*, 7483.
[55] M. Gaborieau, R. G. Gilbert, A. Gray-Weale, J. M. Hernandez, P. Castignolles, *Macromol. Theory Simul.* **2007**, *16*, 13.
[56] R. C. S. Dias, M. R. P. F. N. Costa, ''Calculation of CLD using Population Balance Equations of Generating Functions: Linear and Non-Linear Ideal Controlled Radical Polymerization'', *Macromol. Theory Simul.* **2010**, 19, DOI: 10.1002/mats.201000008.

